Environmental Science & Technology

pubs.acs.org/est

Article

Lake Sediment Archive Reveals a Distinct Response to Anthropogenic Pb and Zn Deposition with Historical Periods: Pb−Zn Isotope Evidence

Yafei Xia, Yuhui Liu, Chengshuai Liu,* Ting Gao, Runsheng Yin, Meng Qi, and Hongchen Wu

Cite This: *Environ. Sci. Technol.* 2023, 57, 15184−15192

Read Online

ACCESS | Metrics & More | Article Recommendations | Supporting Information

ABSTRACT: Anthropogenic activities release large quantities of heavy metals into the atmosphere. In China, the input of these heavy metals through local and trans-boundary atmospheric deposition is poorly understood. To assess this issue, herein, we use Pb and Zn isotopes to constrain the sources of Pb and Zn in a ^{210}Pb-dated sediment core collected from the enclosed lake in South China. We observed a progressive shift toward higher ^{208}Pb/^{206}Pb and Pb fluxes (0.79−4.02 $\mu g \cdot cm^{-2} \cdot a^{-1}$) from 1850 to 1950 and a consistent decrease in $\delta^{66}Zn_{IRMM}$ (as low as −0.097 ± 0.030‰) coupled with an increase in Pb (1.74−3.36 $\mu g \cdot cm^{-2} \cdot a^{-1}$) and Zn (8.07−10.44 $\mu g \cdot cm^{-2} \cdot a^{-1}$) fluxes after 1980. These distinguished isotopic signals and flux variations reveal the presence of trans-boundary Pb since 1900, with the addition of local industrial Pb and Zn pollution after 1980. Up to 72.3% of Pb deposited at our site can be attributed to long-distance transportation from previously industrialized countries, resulting in a noteworthy legacy of Pb in China since 1900. Despite the phasing out of leaded gasoline, Chinese gasoline still contributes an average of 20.9%. The contribution of China's mining and smelting activities to Pb has increased steadily since 1980 and remained stable at an average of 25.1% since 2000.

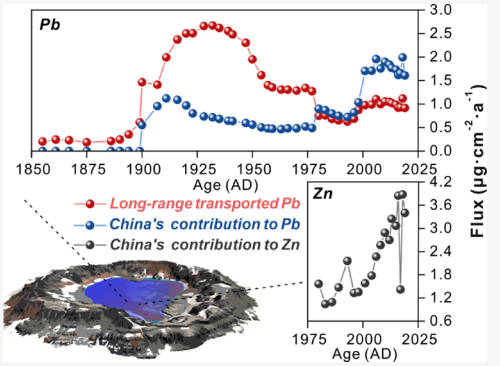

KEYWORDS: *long-distance transportation, anthropogenic activities, sediment core, atmospheric heavy metals, isotopes*

1. INTRODUCTION

Since the Industrial Revolution in the 1800s, growing anthropogenic activities and industrial development have accelerated the consumption of fossil fuels and mineral resources, resulting in a substantial release of associated pollutants into the environment.[1] Among various pollutants emitted by anthropogenic activities, volatile heavy metals such as Pb and Zn are the most concerning owing to their long-range transport in the atmosphere and persistent toxicity to ecosystems and human health.[2−4] Currently, even Earth's most remote areas (such as the polar and alpine regions) are facing risks of Pb and Zn pollution caused by the atmospheric deposition of these heavy metals.[5−7] Historically released Pb and Zn also have far-reaching impacts on the environment due to their persistent toxicity. The anthropogenic emissions of Pb and Zn have been observed to fluctuate over time in different countries.[8−11] In general, the industrial structure and the economic growth rates of a country determine its category and intensity of emissions, respectively.[12,13] However, the historical Pb and Zn pollution sources of a country are often hard to determine because these heavy metals can be transported long distances from their sources.

The international community has held China accountable for its coeval emission of heavy metals into the global atmosphere since its rapid industrialization in the 1980s.[14,15] However, this remains debatable because before its industrialization, China had experienced trans-boundary atmospheric heavy metal deposition from other areas.[16,17] The impact of industrial development on Pb and Zn emissions in China can be solved by investigating the historical records of Pb and Zn in natural archives. Sediment cores collected from enclosed lakes can undertake this task, given that these lakes receive materials mainly via atmospheric deposition with limited contribution from the ambient surface due to small watersheds.[18,19] The chronology of sediment cores can be precisely established via ^{210}Pb dating.[20,21] Multiplying metal concentrations by their sedimentation rates can yield an influx of metals into lakes.[22] Studies of ^{210}Pb-dated sediment cores worldwide have observed peaks in Pb or Zn concentrations and influxes over the past decades, indicative of enhanced atmospheric deposition resulting from industrialization.[4,23−25] Although some researchers have observed long-range crossovers, their contributions remain unclear.[24,26]

Received: January 19, 2023
Revised: September 3, 2023
Accepted: September 5, 2023
Published: September 18, 2023

Stable isotopes can offer valuable insights into the origins of substances and have proven to be effective tools for both quantitative and qualitative analyses.[27,28] However, revealing the origins of atmospheric deposition of both Pb and Zn solely on the basis of a single isotope ratio is challenging due to the asynchrony in emissions. Moreover, using a single isotope system may not suffice for accurately apportioning multiple sources, as there could be overlapping isotopic compositions among different sources.[27,28] Multiple isotope analysis offers a promising multidimensional approach for assessing sources in complex systems, thereby addressing these obstacles.[29] Pb isotopes have been widely used as a tool to identify Pb sources, due to their stability during epigenetic geochemical processes.[30] The Pb isotopes in sediments[19,31] and peat bogs[32,33] have proven very effective for identifying atmospheric Pb; however, drawbacks persist due to the presence of overlapping Pb isotopes originating from diverse sources.[2] The use of Zn isotope compositions, in addition to Pb, is beneficial because unlike Pb, they can be influenced by a variety of different processes.[34] For example, high-temperature processes like smelting can induce distinct fractionation of Zn isotopes, resulting in a lighter isotopic composition of atmospheric Zn.[35,36] The use of Zn isotopes can thus serve as a complementary method to Pb isotopes for distinguishing atmospheric sources.[28,34] The incorporation of an alternative isotope system enables improved source discrimination in cases where isotopic signatures from diverse origins overlap. Therefore, the two different isotope systems are complementary and can offer diverse information to discriminate Pb and Zn inputs from local and trans-boundary atmospheric deposition pathways.

We extracted a sediment core from a closed Maar Lake in southern China to reconstruct Pb and Zn deposition histories and understand their sources since the Industrial Revolution. Correspondingly, we combined Pb−Zn geochemistry, sedimentary chronology, and Pb−Zn isotopic measurements to (1) obtain the deposition fluxes of Pb and Zn at various historical stages, (2) link the deposition trends of Pb and Zn with emission sources corresponding to the evolution of global anthropogenic activity, and (3) quantify the contribution of anthropogenic emissions to Pb and Zn accumulation. The combined utilization of Pb and Zn isotopes reveals distinct pollution histories for each metal, thus providing crucial insights into the extent of historical heavy metal contamination resulting from both local and trans-boundary atmospheric deposition. Accordingly, these findings provide the first assessment of atmospheric Pb and Zn sources in southern China over the past 2 centuries.

2. MATERIALS AND METHODS

2.1. Geographic Information. Huguangyan Maar Lake is located in the northern Leizhou Peninsula of Guangdong Province, China (110°17′06″E, 21°08′40″N; Figure 1), which is one of the earliest and most developed regions in China. The lake has a small ratio of catchment area (3.2 km^2) to lake area (2.25 km^2), which is surrounded by pyroclastic basalt rock with no nearby rivers or streams.[37] This indicates that the lake receives Pb and Zn mostly via atmospheric deposition. The relative flatness of the lake basin and the stability of the body of water favor the formation and preservation of deposition records.[38] This region is located on the coastline of South China and in the tropical convergence zone and the subtropical-tropical transition zone, which is dominated by

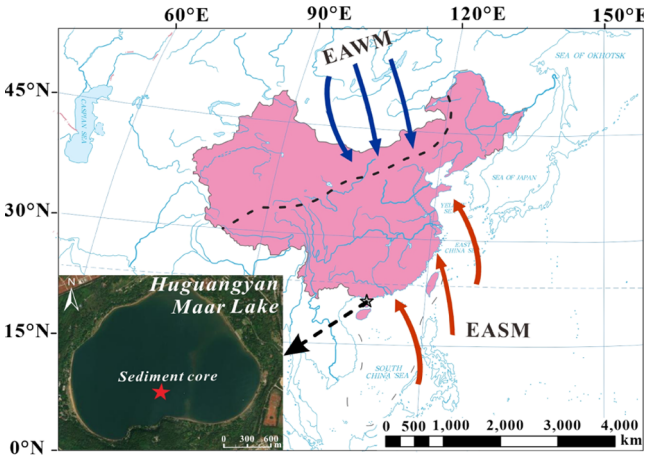

Figure 1. Map of the study area and location of the sampling site. East Asian monsoon systems: The East Asian Summer Monsoon (EASM) prevails in the summer, while the East Asian Winter Monsoon (EAWM) prevails in winter.

the East Asian summer monsoon in summer and the East Asian winter monsoon in winter.[37,39] The atmospheric deposition of heavy metals from high-latitude West European or North American regions could be transported to middle-latitude East Asian regions through the interaction of the Westerlies with East Asian monsoon.[40,41] Thus, the unique location and geography of the lake provide valuable insights into the history of the atmospheric deposition of Pb−Zn and their local and global sources.[42−44]

2.2. Sample Description. An 82 cm sediment core was collected from the middle of Huguangyan Maar Lake in August 2020 using a free-fall gravity sampler. The sediment core was sliced into 1.0 cm intervals in the field and transported to the laboratory in 50 mL centrifuge tubes. In the laboratory, samples were freeze-dried and powdered (<63 μm) prior to chemical analyses. The chronology of our samples is based on ^{210}Pb dating of a 78 cm sediment core collected at the same site and the same time, which has been reported in detail in our most recent study.[45] The results of the chronology for each sample depth representation calculated according to the constant flux and constant sedimentation rate (CFCS) model are listed in Table S1.

2.3. Metal Concentration Analyses. Before the samples were analyzed for their metal concentrations, they were completely digested with concentrated acid (HCl−HNO_3−HF), as detailed in the Supporting Information. Metal concentrations were determined by inductively coupled plasma optical emission spectroscopy (PerkinElmer Optima 8000), as well as inductively coupled plasma-mass spectrometry (PlasmaQuant-MS Elite, Germany). A multielement standard solution was used to build the calibration curve. Blank samples and geological reference material (AGV-2) were used for quality control. The relative standard deviations (RSDs) of our measurements were less than 2% for major element analyses and 10% for trace element concentration measurements.

2.4. Pb Purification and Isotope Analysis. Pure Pb solution was separated by chromatographic columns in a class-1000 clean room equipped with class-100 laminar flow hoods at the Guangdong Institute of Eco-environmental Science & Technology, Guangzhou, China. HCl, HBr, and HF were distilled twice by sub-boiling distillation (Savillex), and all wares used in sample preparation were cleaned following a

https://doi.org/10.1021/acs.est.3c00511
Environ. Sci. Technol. 2023, 57, 15184−15192

strict procedure to ensure that the total Pb procedure blank for the whole analyses was less than ~3 pg per analysis. Pb purification was conducted using anion exchange resin (AG1-X8, 200−400 mesh, Bio-Rad) (details are available in the Supporting Information).

Pb isotope ratios of all samples were measured on a Neptune Plus multicollector inductively coupled plasma-mass spectrometer (MC-ICP-MS, Thermo Scientific) at the Institute of Geochemistry, Chinese Academy of Sciences, China. NIST 981 solution was diluted to ~50 ppb in 3% HNO_3 (m/m) with ~10 ppb of thallium standard (Tl; NIST 997) added as an internal standard for mass fractionation correction ($^{205}Tl/^{203}Tl$ = 2.3871). The obtained values of NIST 981 were 2.1667 ± 0.0012 (2 times standard deviations (2SD), N = 57) and 1.0934 ± 0.0002 (2SD, N = 57) for $^{208}Pb/^{206}Pb$ and $^{206}Pb/^{207}Pb$, respectively, and agree with other references.[30,46] The $^{208}Pb/^{206}Pb$ and $^{206}Pb/^{207}Pb$ ratios of the geological reference material BCR-2 were 2.0644 and 1.1995, respectively, which were similar to previously reported data (2.0620 ± 0.0147 and 1.1959 ± 0.0086, respectively).[47]

2.5. Zn Purification and Isotope Analysis. Pure Zn solution was separated in the same ultraclean experimental environment as Pb by chromatographic columns using the anion exchange resin AG MP-1M (100−200 mesh, Bio-Rad) according to the procedure of Lv et al. and our previous studies[48,49] given in the Supporting Information. The same column procedure was repeated to obtain a further purified Zn solution for isotopic analyses.

Zn isotope analysis was also carried out on the MC-ICP-MS using wet plasma and the sample-standard bracketing (SSB) method.[50] The Zn isotope compositions of the samples were reported relative to the standard Institute of Reference Materials and Measurement (IRMM)-3702 using δ notation based on the $^{66}Zn/^{64}Zn$ ratio expressed as $\delta^{66}Zn_{IRMM} = [(^{66}Zn/^{64}Zn)_{sample}/(^{66}Zn/^{64}Zn)_{IRMM} - 1] \times 1000$. The total procedural blanks (from sample dissolution to mass spectrometry) were routinely measured and had a long-term average of less than 2% for Zn, which is considered neglected during mass spectrometry. The geological reference materials BCR-2 and AGV-2 yielded average $\delta^{66}Zn_{IRMM}$ values of −0.039 ± 0.035‰ (2SD, N = 3) and −0.044 ± 0.022‰ (2SD, N = 3), respectively, which were consistent within uncertainty with those reported previously.[51,52]

2.6. Data Calculations. The sediment accumulation rate calculated based on the CFCS model is approximately 0.0625 $g{\cdot}cm^{-2}{\cdot}a^{-1}$ (Text S4). The results for the fluxes of Zn and Pb, calculated by multiplying the mass concentration by the sediment accumulation rate, are given in Table S2. Enrichment factors (EFs) normalized by Al (aluminum) were used to assess the enrichment and pollution. The details of the calculation are provided in Text S4. The MixSIAR Bayesian isotope mixing model is used to quantify the contribution of different sources to a mixture, which allows the calculation of contributions from more than three sources and explicitly accounts for uncertainties in the isotopic values.[53] More details on calculations are presented in the Supporting Information.

3. RESULTS AND DISCUSSION

3.1. Temporal Patterns in Pb and Zn. The Pb flux shows a background value (average 0.72 $\mu g{\cdot}cm^{-2}{\cdot}a^{-1}$) before 1850, followed by a rapid increase prior to reaching a peak value of 4.02 $\mu g{\cdot}cm^{-2}{\cdot}a^{-1}$ in approximately 1920, a gradual decrease from the 1920s to the 1980s, and a new peak after the 2000s (Figure 2 and Table S2). The Pb isotope ratios show a revised trend with Pb fluxes (Figure 2). This Pb record presented here

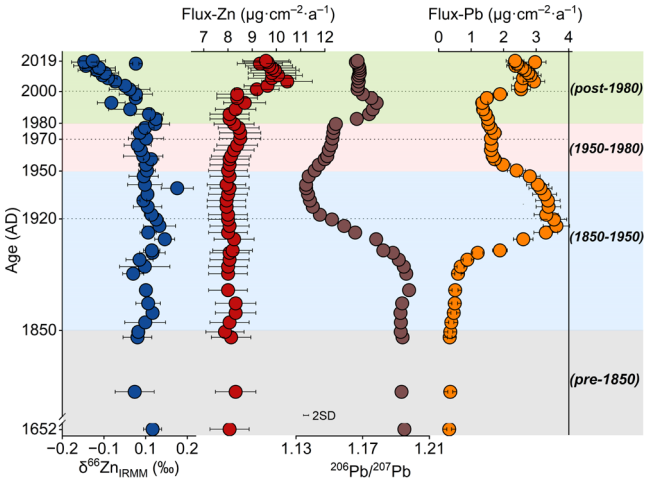

Figure 2. Temporal variations in Zn flux, $\delta^{66}Zn_{IRMM}$, Pb flux, and $^{206}Pb/^{207}Pb$ (error bars reflect ±2SD of NIST 981) in the sediment core. Four stages were divided according to Pb and Zn temporal variations: pre-1850, 1850−1950, 1950−1980, and post-1980.

is consistent with previous observations in southern China.[45,54] The similar records of Pb show a highly consistent pattern of Pb deposition from preindustrial to industrial times, suggesting a deeply coherent signature of Pb under small- to large-scale anthropogenic release of Pb into the atmosphere. Zn shows a distinct distribution pattern from Pb (Figure 2). Zn fluxes range from 7.88 to 10.44 $\mu g{\cdot}cm^{-2}{\cdot}a^{-1}$, with slight fluctuations before 1950, followed by a slow increase from 1950 to 1980, a rapid increase from 1980 to 2000, and a slow decrease after the 2000s (Figure 2 and Table S2). Notably, Zn isotope ratios also exhibit a revised trend with respect to Zn fluxes. A similar vertical distribution of Zn was also observed in the lake sediments collected from southern China and Mongolia,[31,45,55] indicating low Zn deposition before 1980 and a continuous increase after 1980. By combining the vertical characteristics of Pb and Zn, the sedimentary core can be divided into four stages: pre-1850, 1850−1950, 1950−1980, and post-1980 (Figure 2).

3.2. Preindustrial Levels of Pb and Zn before 1850. Before 1850, the Pb and Zn fluxes were remarkably stable, with average values of 0.72 and 8.07 $\mu g{\cdot}cm^{-2}{\cdot}a^{-1}$, respectively (Figure 2 and Table S2). The consistently low Pb and Zn fluxes in the pre-1850 samples, with EF values of ~1 for both metals (Figure S1), indicate that the pollution levels of these metals were low before the 1850s. This is consistent with the fact that production of Pb and Zn before 1850 was low, resulting in minimal atmospheric pollution.[56] Thus, Pb and Zn in the pre-1850 samples are likely to originate from natural sources, as indicated by their isotopic signals (Figure 3).

Due to the limited Zn isotope fractionation caused by basalt weathering,[57] the Zn isotope composition of the deepest sediments (from 0.024 ± 0.047‰ to 0.086 ± 0.026‰) was comparable to that of the unweathered basalt (0.03 ± 0.02‰) (Table S2). Correspondingly, the current data demonstrate that there was no (almost negligible) fractionation of Zn isotopes in lakes as a result of natural processes and variations in $\delta^{66}Zn_{IRMM}$ may serve as an excellent indicator of possible Zn sources. Although speculative at best, we propose that the low

https://doi.org/10.1021/acs.est.3c00511
Environ. Sci. Technol. 2023, 57, 15184−15192

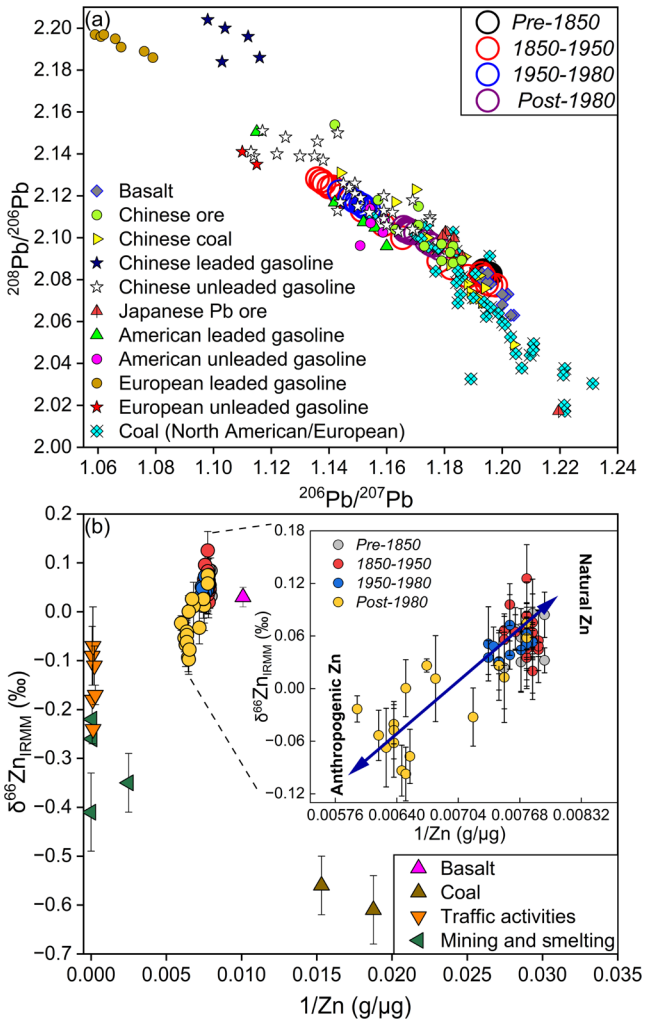

Figure 3. (a) Diagram of $^{206}Pb/^{207}Pb$ versus $^{208}Pb/^{206}Pb$ in the sediment core. Compilation of $^{206}Pb/^{207}Pb$ versus $^{208}Pb/^{206}Pb$ in possible sources of deposition (data obtained from Table S3). (b) $\delta^{66}Zn_{IRMM}$ versus 1/Zn for all lake sediments and possible anthropogenic sources (data obtained from Table S4).

ionic strength, low perturbation, and high degree of anaerobic conditions in the deep lake, which reduce the mobility of diffusing ions, are likely to limit the fractionation of Zn isotopes.[44] This phenomenon has also been reported for the sediment cores obtained from the United States, where the authors hypothesized that the transport and biogeochemical cycling of Zn have little impact on the Zn isotopic signature of lake sediments.[11] Additionally, conservative Zn isotopes were observed in anaerobic sediments within coastal environments since Zn isotopic signatures remain nearly unaltered during the transport associated with suspended particulate matter and by postdepositional processes.[58,59] As biogeochemical processes typically have minimal impact on the Zn isotope compositions of sediments, the consistency of Zn isotopes as a conservative source tracer is supported.[60,61]

3.3. Pb and Zn Sources from 1850 to 1950. The Pb flux gradually increased after the 1850s and reached a maximum (~4.02 $\mu g \cdot cm^{-2} \cdot a^{-1}$) around the 1920s until 1950, showing an increase of 6 times compared with the pre-1850 period (Figure 2 and Table S2). The rapid increase in Pb levels from 1850 to 1920 and the high Pb peak around 1920 suggest severe Pb pollution (Figure 2). Given that China did not experience large-scale industrialization at this time, Pb pollution could be attributed to the deposition of atmospheric Pb transported over long distances from other regions. Since ~1860, the Second Industrial Revolution has facilitated rapid industrialization in countries such as the United States, Germany, the United Kingdom, France, Italy, and Japan. Therefore, Pb was extensively released into the atmosphere due to fossil fuel combustion and metal production.[13] The rise in Pb pollution observed in Greenland ice has tracked the rapid expansion of coal consumption in Europe and North America in the late 19th century.[62] Japan released considerable amounts of Pb in the 1900s due to the use of domestic and imported ores (Canada and Australia) in Pb smelting, as well as the consumption of leaded gasoline.[4,63,64] Notably, all leaded gasoline used in Japan was imported from the United States and the United Kingdom.[65] The tetraethyl Pb was added to 90% of gasoline in the United States by 1936,[62] and the use of Pb (mainly tetraethyl Pb) as gasoline additives contributed to the increase in Pb pollution in Japan since the 1920s. The reduction in Pb flux observed in our sediment from the 1920s to 1950 (Figure 2) may be attributed to a 30% decline in coal consumption in the United States between 1920 and 1935.[66] The long-distance atmospheric transport of Pb during this period has resulted in a coeval change in Pb levels in Greenland ice core.[62] The $^{206}Pb/^{207}Pb$ values of our samples during 1850 and 1950 support the origin of Pb from the earlier industrialized regions (Figure 3a). Based on the above discussion, we estimated the contribution of these sources using a Bayesian model. The Pb isotope ratios of the sources are listed in Table S5, and the details of the model calculations are presented in Text S4. With the introduction of anthropogenic activity, the contribution of natural sources decreased from ~70 to ~10% from 1850 to 1950. In addition, long-distance transportation contributed 26.2% of Pb to sediments from 1850 to 1900 (from coal and ore), and this contribution increased by 60.1% between 1900 and 1950 due to the use of leaded gasoline (Figure 4 and Table S6).

Significant enrichment differences existed between Pb and Zn, with Pb being 2−6 orders of magnitude more contaminated than Zn during this period (Figure S1). The

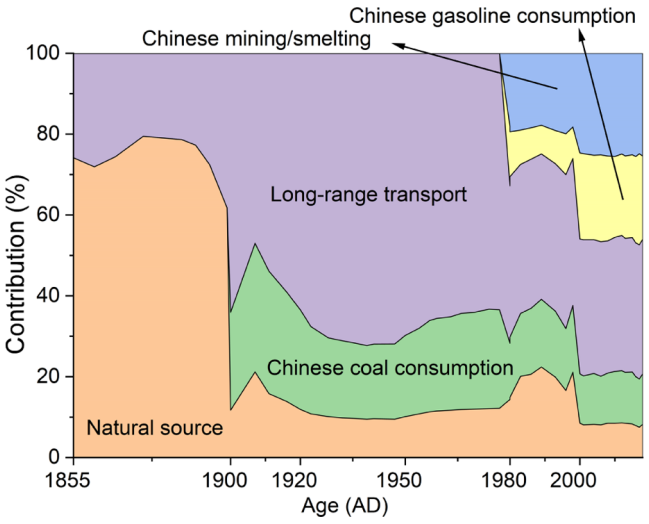

Figure 4. Contributions calculated using $^{208}Pb/^{206}Pb$ and $^{206}Pb/^{207}Pb$ by the MixSIAR Bayesian isotope mixing model (data presented in Table S5).

https://doi.org/10.1021/acs.est.3c00511
Environ. Sci. Technol. 2023, 57, 15184−15192

absence of Zn flux peaks between 1850 and 1950 suggests that Pb and Zn sources differed during this period (Figure 2). In addition, the presence of similar $\delta^{66}Zn_{IRMM}$ values between 1850 and 1950 and the pre-1850 samples (0.03 ± 0.02‰) suggests that Zn was sourced from local silicate weathering during this period (Figure 3b). The combustion of leaded gasoline during 1850−1950, the primary source of Pb (accounting for up to 53%; Figure 4 and Table S3), is unlikely to have resulted in substantial Zn emissions. In addition, industries closely linked to Zn emissions in the atmosphere were likely to be in their early stages, as indicated by the relatively low global annual Zn production (<3 Mt·a^{-1}) between 1850 and 1950.[67]

3.4. Low-Intensity Pb and Zn Emissions from China during 1950−1980. Pb changed slightly during 1950−1980, with fluxes decreasing from 2.80 to 1.93 μg·cm^{-2}·a^{-1} and $^{206}Pb/^{207}Pb$ increasing from 1.1411 to 1.1538, respectively (Figure 2 and Table S2). Based on our findings, the early stage of China during 1950−1980 was characterized by low levels of Pb and Zn contamination (Figure 2), although EF values of Pb were still almost 2 times higher than those during the preindustrial period (Figure S1). This could be explained by the fact that consumption of fossil fuels was low, and industrialization should have been severely limited during this period.[56] This is further supported by the absence of a Zn peak from 1950 to 1980 (Figure 2). In addition, $\delta^{66}Zn_{IRMM}$ values during this period support local silicate weathering rather than local nonferrous metal mining and other industrial sources (Figure 3b). Notably, Pb emissions in China (<2500 t·a^{-1}) during this period are considerably lower than the maximum historical Pb emissions in the USA (~200,000 t·a^{-1}), Europe (~100,000 t·a^{-1}), and Russia (~50,000 t·a^{-1}),[13] implying that industrial recovery in this period is not likely to have resulted in a comparable environmental Pb burden. Given the low degrees of industrialization in China, we can, therefore, conclude that Pb in this period mainly originated from the long-distance transport of atmospheric Pb from other regions. A decline in Pb was also observed at numerous sites worldwide, most likely as a result of the implementation of cleaner production standards and the elimination of leaded gasoline in Europe and North America.[14,68,69] Based on the Bayesian model, the contribution of Pb from long-range transport decreased to 62.9% between 1950 and 1980, with the addition of Chinese coal contributing 22.1% (Figure 4 and Table S6).

3.5. Economic Reform Enhanced Industrial Pb and Zn Emissions from China after 1980. In the early 1980s, China implemented the "Reform and Opening-up" policy, which led to a considerable increase in industrial activities and economic growth.[45] We observed a coupled and rapid increase in the flux of Pb and Zn in our samples, suggesting that considerable anthropogenic emissions of Zn and Pb occurred during this period (Figure 2). Benefiting from the Economic Reform policy, the efficiency and enthusiasm of Chinese society were largely enhanced.[70] During this period, China experienced substantial economic growth and industrialization associated with a huge demand for mineral resources.[67,71] As one of the most developed provinces in China, Guangdong Province experienced economic growth, rapid population growth, massive construction, and urban sprawl in the post-1980 period, during which both Pb and Zn experienced corresponding bulk growth due to their crucial applications within industrialization.[72] Mining, refining, and exploitation of mineral resources were highly active in China during this stage. This could explain the covariation of Pb and Zn in our samples as these two metals are associated with each other in many mineral deposits.[73] The co-increase in Pb and Zn also agrees with the rapid growth rate (≥10%) of annual gross domestic product in China after 1980,[70] suggesting that the economic growth of China might lead to pollution of the surrounding environment to large degrees.[13]

After 1980, the Pb flux increased, peaking at 3.36 μg·cm^{-2}·a^{-1}, while the $^{206}Pb/^{207}Pb$ ratios decreased slightly from 1980 to 2000 and have remained constant since 2000 (Figure 2 and Table S2). As observed in Figure 3a, the Pb isotope trace map indicates the influence of mining/smelting and gasoline. Furthermore, calculations based on the Bayesian model show that the long-range transport contribution declined from 62.9 to 34.9% following the phasing out of leaded gasoline in the United States and Europe in the 1970s. Thus, after the year 2000, atmospheric Pb was characterized by stable contributions from various sources of pollution, with average contributions of 9.2, 33.4, 12.7, 20, and 24.0% from natural sources, long-range transport, Chinese coal consumption, Chinese gasoline consumption, and Chinese mining/smelting activities, respectively (Figure 4 and Table S6). The as-observed relative stability of the sources may be attributable to the development of environmental protection in China after the 1980s, such as the overhaul and closure of heavy industry enterprises and the ban on leaded gasoline in 2000. This is supported by the fact that $^{206}Pb/^{207}Pb$ decreased slightly between 1980 and 2000 and has remained stable since 2000 (Figure 2). However, it is worth noting that even when the Pb flux was reduced, the EF of Pb in the sediment remained significantly greater than 1 (Figure S1). In addition, the monitoring data revealed that the flux of Pb in atmospheric aerosol samples in Shanghai and Tianjin remained high, despite a slight downward trend following the phasing out of leaded gasoline.[74,75] This is a cautionary tale for our future development, and we should find ways to prevent economic growth based on large metal emissions from becoming a potential environmental threat.

Zn flux also continued to increase, with an elevated average value of 9.27 μg·cm^{-2}·a^{-1} after 1980. There is also a clear transition of Zn isotopes in which $\delta^{66}Zn_{IRMM}$ gradually decreases upward from 0.073 ± 0.035‰ to values as low as −0.097 ± 0.030‰ (Figure 2 and Table S2). A recent study suggests that the enrichment of light Zn isotopes in sediments is due to the biological uptake and transport of organically bound light Zn to sediments during biomass mineralization.[76] However, the lake investigated in the aforementioned study experienced a century of intense eutrophication and increased biological activity. This condition differs from that of our subtropical oligotrophic lake, where primary production was low,[77,78] most likely decreasing the degree of Zn fractionation as a result of biological uptake. Previous studies have also demonstrated that lighter Zn isotopes are preferentially integrated into atmospheric emissions during high-temperature processes.[27,79] For example, anthropogenic Zn from urban and industrial atmospheric emissions, primarily released by smelting and mining,[48,80,81] vehicular traffic,[8,82,83] and coal combustion,[84] exhibits lighter isotope compositions ranging from −0.41 to −0.22‰, −0.24 to −0.07‰, and −0.61 to −0.56‰, respectively (Table S4). Herein, the linear correlation between the $\delta^{66}Zn_{IRMM}$ values and 1/Zn could be attributed to binary mixing between a natural source with a

https://doi.org/10.1021/acs.est.3c00511
Environ. Sci. Technol. 2023, 57, 15184−15192

higher $\delta^{66}Zn_{IRMM}$ value and an anthropogenic source with a lower $\delta^{66}Zn_{IRMM}$ value (Figure 3b). Consequently, this observable Zn shift in the uppermost sediments indicates enhanced anthropogenic contamination since 1980. The relative contributions of different sources after 1980 were determined similarly using the Bayesian model based on the Zn isotopes. The results demonstrate an increasing anthropogenic contribution, ranging from 9.1 to 39.9%, with a mean value of 21.7% (Figure S3 and Table S7).

■ ASSOCIATED CONTENT

Supporting Information

The Supporting Information is available free of charge at https://pubs.acs.org/doi/10.1021/acs.est.3c00511.

Additional analytical details, methods, figures, and tables (PDF)

■ AUTHOR INFORMATION

Corresponding Author

Chengshuai Liu − *State Key Laboratory of Environmental Geochemistry, Institute of Geochemistry, Chinese Academy of Sciences, Guiyang 550081, P. R. China; CAS Center for Excellence in Quaternary Science and Global Change, Xi'an 710061, P. R. China; National-Regional Joint Engineering Research Center for Soil Pollution Control and Remediation in South China, Guangdong Key Laboratory of Integrated Agro-environmental Pollution Control and Management, Guangdong Institute of Eco-environmental and Soil Science, Guangdong Academy of Sciences, Guangzhou 510650, P. R. China;* orcid.org/0000-0003-0133-0119; Phone: +86-13828421192; Email: liuchengshuai@vip.gyig.ac.cn

Authors

Yafei Xia − *State Key Laboratory of Environmental Geochemistry, Institute of Geochemistry, Chinese Academy of Sciences, Guiyang 550081, P. R. China; University of Chinese Academy of Sciences, Beijing 100049, P. R. China*

Yuhui Liu − *State Key Laboratory of Environmental Geochemistry, Institute of Geochemistry, Chinese Academy of Sciences, Guiyang 550081, P. R. China*

Ting Gao − *State Key Laboratory of Environmental Geochemistry, Institute of Geochemistry, Chinese Academy of Sciences, Guiyang 550081, P. R. China*

Runsheng Yin − *State Key Laboratory of Ore Deposit Geochemistry, Institute of Geochemistry, Chinese Academy of Sciences, Guiyang 550081, P. R. China*

Meng Qi − *State Key Laboratory of Environmental Geochemistry, Institute of Geochemistry, Chinese Academy of Sciences, Guiyang 550081, P. R. China; University of Chinese Academy of Sciences, Beijing 100049, P. R. China*

Hongchen Wu − *State Key Laboratory of Environmental Geochemistry, Institute of Geochemistry, Chinese Academy of Sciences, Guiyang 550081, P. R. China*

Complete contact information is available at: https://pubs.acs.org/10.1021/acs.est.3c00511

Author Contributions

Y.X.: investigation, experimentation, data analysis, formal analysis, writing, review and editing. Y.L.: experimentation, data analysis, formal analysis, review and editing. C.L.: supervision, methodology, funding acquisition, review and editing. T.G.: data analysis, formal analysis, review and editing. R.Y.: formal analysis, review and editing. M.Q.: sample collection and processing, review and editing. H.W.: sample collection, data analysis, review and editing.

Notes

The authors declare no competing financial interest.

■ ACKNOWLEDGMENTS

The authors thank Dr. Yang Tang for help in the MC-ICPMS lab. This work was financially supported by the Strategic Priority Research Program of CAS (XDB40020402), the National Natural Science Foundation of China (42025705 and 41921004), Guizhou High-level Talent Project (GCC[2022] 002-1), and the West Light Foundation of The Chinese Academy of Sciences (xbzg-zdsys-201902).

■ REFERENCES

(1) Al Mamun, A.; Cheng, I.; Zhang, L. M.; Dabek-Zlotorzynska, E.; Charland, J. P. Overview of size distribution, concentration, and dry deposition of airborne particulate elements measured worldwide. *Environ. Rev.* **2020**, *28* (1), 77−88.

(2) Bi, X. Y.; Li, Z. G.; Wang, S. X.; Zhang, L.; Xu, R.; Liu, J. L.; Yang, H. M.; Guo, M. Z. Lead Isotopic Compositions of Selected Coals, Pb/Zn Ores and Fuels in China and the Application for Source Tracing. *Environ. Sci. Technol.* **2017**, *51* (22), 13502−13508.

(3) Zhu, B.-Q.; Yu-Wei, C.; Xiang-Yang, C. Application of Pb isotopic mapping to environment evaluation in China. *Chem. Speciation Bioavailability* **2002**, *14* (1−4), 49−56.

(4) Nitzsche, K. N.; Yoshimura, T.; Ishikawa, N. F.; Ogawa, N. O.; Suzuki, K.; Ohkouchi, N. Trace metal geochemical and Zn stable isotope data as tracers for anthropogenic metal contributions in a sediment core from Lake Biwa, Japan. *Appl. Geochem.* **2021**, *134*, No. 105107.

(5) Kenntner, N.; Crettenand, Y.; Funfstuck, H. J.; Janovsky, M.; Tataruch, F. Lead poisoning and heavy metal exposure of golden eagles (Aquila chrysaetos) from the European Alps. *J. Ornithol.* **2007**, *148* (2), 173−177.

(6) McConnell, J. R.; Edwards, R. Coal burning leaves toxic heavy metal legacy in the Arctic. *Proc. Natl. Acad. Sci. U.S.A.* **2008**, *105* (34), 12140−12144.

(7) Angot, H.; Dastoor, A.; De Simone, F.; Gardfeldt, K.; Gencarelli, C. N.; Hedgecock, I. M.; Langer, S.; Magand, O.; Mastromonaco, M. N.; Nordstrom, C.; Pfaffhuber, K. A.; Pirrone, N.; Ryjkov, A.; Selin, N. E.; Skov, H.; Song, S. J.; Sprovieri, F.; Steffen, A.; Toyota, K.; Travnikov, O.; Yang, X.; Dommergue, A. Chemical cycling and deposition of atmospheric mercury in polar regions: review of recent measurements and comparison with models. *Atmos. Chem. Phys.* **2016**, *16* (16), 10735−10763.

(8) Cloquet, C.; Carignan, J.; Libourel, G. Isotopic composition of Zn and Pb atmospheric depositions in an urban/periurban area of northeastern France. *Environ. Sci. Technol.* **2006**, *40* (21), 6594−6600.

(9) Hatano, N.; Yoshida, K. Vertical and horizontal distribution of sedimentary facies and hydromorphic paleosols around paleo-lake in the Pliocene sediments in southwest Japan. *Catena* **2020**, *187*, No. 104387.

(10) Li, J.; Wang, L.; Zou, Y.; Li, J. Spatial variation of diatom diversity with water depth at Huguang Maar Lake, Southern China. *J. Paleolimnol.* **2022**, *68* (1), 119−131.

(11) Thapalia, A.; Borrok, D. M.; Van Metre, P. C.; Wilson, J. Zinc isotopic signatures in eight lake sediment cores from across the United States. *Environ. Sci. Technol.* **2015**, *49* (1), 132−140.

(12) Cooke, C. A.; Martinez-Cortizas, A.; Bindler, R.; Gustin, M. S. Environmental archives of atmospheric Hg deposition - A review. *Sci. Total Environ.* **2020**, *709*, No. 134800, DOI: 10.1016/j.scitotenv.2019.134800.

(13) Marx, S. K.; Rashid, S.; Stromsoe, N. Global-scale patterns in anthropogenic Pb contamination reconstructed from natural archives. *Environ. Pollut.* **2016**, *213*, 283−298.

(14) Koffman, B. G.; Saylor, P.; Zhong, R.; Sethares, L.; Yoder, M. F.; Hanschka, L.; Methven, T.; Cai, Y.; Bolge, L.; Longman, J.; Goldstein, S. L.; Osterberg, E. C. Provenance of Anthropogenic Pb and Atmospheric Dust to Northwestern North America. *Environ. Sci. Technol.* **2022**, *56* (18), 13107−13118.
(15) Liu, J.; Diamond, J. China's environment in a globalizing world. *Nature* **2005**, *435* (7046), 1179−1186.
(16) Shotyk, W.; Weiss, D.; Appleby, P. G.; Cheburkin, A. K.; Frei, R.; Gloor, M.; Kramers, J. D.; Reese, S.; Van der Knaap, W. O. History of atmospheric lead deposition since 12,370 C-14 yr BP from a peat bog, Jura Mountains, Switzerland. *Science* **1998**, *281* (5383), 1635−1640.
(17) Nriagu, J. O. A history of global metal pollution. *Science* **1996**, *272* (5259), 223−224.
(18) Gravina, P.; Ludovisi, A.; Moroni, B.; Vivani, R.; Selvaggi, R.; Petroselli, C.; Cappelletti, D. Geochemical Proxies and Mineralogical Fingerprints of Sedimentary Processes in a Closed Shallow Lake Basin Since 1850. *Aquat. Geochem.* **2022**, *28* (1), 43−62.
(19) Thevenon, F.; Guédron, S.; Chiaradia, M.; Loizeau, J.-L.; Poté, J. (Pre-) historic changes in natural and anthropogenic heavy metals deposition inferred from two contrasting Swiss Alpine lakes. *Quat. Sci. Rev.* **2011**, *30* (1−2), 224−233.
(20) Sahoo, P. K.; Guimarães, J. T. F.; Souza-Filho, P. W. M.; Powell, M. A.; da Silva, M. S.; Moraes, A. M.; Alves, R.; Leite, A. S.; Júnior, W. N.; Rodrigues, T. M.; Costa, V. E.; Dall'Agnol, R. Statistical analysis of lake sediment geochemical data for understanding surface geological factors and processes: An example from Amazonian upland lakes, Brazil. *Catena* **2019**, *175*, 47−62.
(21) Zhu, T.; Wang, X.; Lin, H.; Ren, J.; Wang, C.; Gong, P. Accumulation of Pollutants in Proglacial Lake Sediments: Impacts of Glacial Meltwater and Anthropogenic Activities. *Environ. Sci. Technol.* **2020**, *54* (13), 7901−7910.
(22) Yin, R. S.; Guo, Z. G.; Hu, L. M.; Liu, W. C.; Hurley, J. P.; Lepak, R. F.; Lin, T.; Fang, X. B.; Li, X. D. Mercury Inputs to Chinese Marginal Seas: Impact of Industrialization and Development of China. *J. Geophys. Res.* **2018**, *123* (8), 5599−5611.
(23) Hillman, A. L.; Abbott, M. B.; Yu, J. Q.; Bain, D. J.; Chiou-Peng, T. Environmental Legacy of Copper Metallurgy and Mongol Silver Smelting Recorded in Yunnan Lake Sediments. *Environ. Sci. Technol.* **2015**, *49* (6), 3349−3357.
(24) Neupane, B.; Kang, S.; Chen, P.; Zhang, Y.; Ram, K.; Rupakheti, D.; Tripathee, L.; Sharma, C. M.; Cong, Z.; Li, C.; Hou, J.; Xu, M.; Thapa, P. Historical Black Carbon Reconstruction from the Lake Sediments of the Himalayan-Tibetan Plateau. *Environ. Sci. Technol.* **2019**, *53* (10), 5641−5651.
(25) Hernández, E.; Obrist-Farner, J.; Brenner, M.; Kenney, W. F.; Curtis, J. H.; Duarte, E. Natural and anthropogenic sources of lead, zinc, and nickel in sediments of Lake Izabal, Guatemala. *J. Environ. Sci.* **2020**, *96*, 117−126.
(26) Aebischer, S.; Cloquet, C.; Carignan, J.; Maurice, C.; Pienitz, R. Disruption of the geochemical metal cycle during mining: Multiple isotope studies of lake sediments from Schefferville, subarctic Québec. *Chem. Geol.* **2015**, *412*, 167−178.
(27) Wang, L.; Jin, Y.; Weiss, D. J.; Schleicher, N. J.; Wilcke, W.; Wu, L.; Guo, Q.; Chen, J.; O'Connor, D.; Hou, D. Possible application of stable isotope compositions for the identification of metal sources in soil. *J. Hazard. Mater.* **2021**, *407*, No. 124812.
(28) Wiederhold, J. G. Metal stable isotope signatures as tracers in environmental geochemistry. *Environ. Sci. Technol.* **2015**, *49* (5), 2606−2624.
(29) Thapalia, A.; Borrok, D. M.; Van Metre, P. C.; Musgrove, M.; Landa, E. R. Zn and Cu Isotopes as Tracers of Anthropogenic Contamination in a Sediment Core from an Urban Lake. *Environ. Sci. Technol.* **2010**, *44* (5), 1544−1550.
(30) He, B.; Zhao, X.; Li, P.; Liang, J.; Fan, Q.; Ma, X.; Zheng, G.; Qiu, J. Lead isotopic fingerprinting as a tracer to identify the pollution sources of heavy metals in the southeastern zone of Baiyin, China. *Sci. Total Environ.* **2019**, *660*, 348−357.
(31) Li, K.; Liu, E. F.; Zhang, E. L.; Li, Y. L.; Shen, J.; Liuc, X. Q. Historical variations of atmospheric trace metal pollution in Southwest China: Reconstruction from a 150-year lacustrine sediment record in the Erhai Lake. *J. Geochem. Explor.* **2017**, *172*, 62−70.
(32) Novák, M.; Emmanuel, S.; Vile, M. A.; Erel, Y.; Veron, A.; Paces, T.; Wieder, R. K.; Vanecek, M.; Stepanova, M.; Brizova, E.; Hovorka, J. Origin of lead in eight central European peat bogs determined from isotope ratios, strengths, and operation times of regional pollution sources. *Environ. Sci. Technol.* **2003**, *37* (3), 437−445.
(33) Rothwell, J. J.; Taylor, K. G.; Chenery, S. R. N.; Cundy, A. B.; Evans, M. G.; Allottt, T. E. H. Storage and Behavior of As, Sb, Pb, and Cu in Ombrotrophic Peat Bogs under Contrasting Water Table Conditions. *Environ. Sci. Technol.* **2010**, *44* (22), 8497−8502.
(34) Desaulty, A. M.; Petelet-Giraud, E. Zinc isotope composition as a tool for tracing sources and fate of metal contaminants in rivers. *Sci. Total Environ.* **2020**, *728*, No. 138599.
(35) Juillot, F.; Maréchal, C.; Morin, G.; Jouvin, D.; Cacaly, S.; Telouk, P.; Benedetti, M. F.; Ildefonse, P.; Sutton, S.; Guyot, F.; Brown, G. E. Contrasting isotopic signatures between anthropogenic and geogenic Zn and evidence for post-depositional fractionation processes in smelter-impacted soils from Northern France. *Geochim. Cosmochim. Acta* **2011**, *75* (9), 2295−2308.
(36) Shiel, A. E.; Weis, D.; Orians, K. J. Evaluation of zinc, cadmium and lead isotope fractionation during smelting and refining. *Sci. Total Environ.* **2010**, *408* (11), 2357−2368.
(37) Mingram, J.; Schettler, G.; Nowaczyk, N.; Luo, X.; Lu, H.; Liu, J.; Negendank, J. F. W. The Huguang maar lake—a high-resolution record of palaeoenvironmental and palaeoclimatic changes over the last 78,000 years from South China. *Quat. Int.* **2004**, *122* (1), 85−107.
(38) Sheng, M.; Wang, X.; Zhang, S.; Chu, G.; Su, Y.; Yang, Z. A 20,000-year high-resolution pollen record from Huguangyan Maar Lake in tropical−subtropical South China. *Palaeogeogr., Palaeoclimatol., Palaeoecol.* **2017**, *472*, 83−92.
(39) Zeng, Z.; Zhou, X.; Li, Z. Y.; Chen, F. J.; Luo, H. J.; He, G. R.; Deng, Z. Y.; Chen, C. Q.; Lao, Q. B. Influence of Typhoons on Chemical Makeup of Rainwater in Zhanjiang, China. *Aerosol Air Qual. Res.* **2022**, *22* (3), No. 210210, DOI: 10.4209/aaqr.210210.
(40) Zhao, X.; Hou, X.; Du, J.; Fan, Y. Anthropogenic 129I in the sediment cores in the East China sea: Sources and transport pathways. *Environ. Pollut.* **2019**, *245*, 443−452.
(41) Porter, S. C.; Zhisheng, A. Correlation between climate events in the North Atlantic and China during the last glaciation. *Nature* **1995**, *375* (6529), 305−308.
(42) Wang, S.; Lü, H.; Liu, J.; Negendank, J. F. W. The early Holocene optimum inferred from a high-resolution pollen record of Huguangyan Maar Lake in southern China. *Chin. Sci. Bull.* **2007**, *52* (20), 2829−2836.
(43) Zeng, Y.; Chen, J.; Yang, Y.; Wang, J.; Zhu, Z.; Li, J. Huguangyan Maar Lake (SE China): A solid record of atmospheric mercury pollution history in a non-remote region. *J. Asian Earth Sci.* **2017**, *147*, 1−8.
(44) Zhang, P.; Wang, B.; Fan, J.; Yin, J. Experiment and interpretation of geomorphological detection by multi-beam sonar in Huguang-yan Maar Lake. *MATEC Web Conf.* **2019**, *283*, 04004.
(45) Wu, H.; Wang, J.; Guo, J.; Hu, X.; Bao, H.; Chen, J. Record of heavy metals in Huguangyan Maar Lake sediments: Response to anthropogenic atmospheric pollution in Southern China. *Sci. Total Environ.* **2022**, *831*, No. 154829.
(46) Wang, C.; Wang, J.; Zhao, Y.; Zhong, C. The vertical migration and speciation of the Pb in the paddy soil: A case study of the Yangtze River Delta, China. *Environ. Res.* **2019**, *179* (Pt A), No. 108741.
(47) Mihaljevič, M.; Baieta, R.; Ettler, V.; Vaněk, A.; Kříbek, B.; Penížek, V.; Drahota, P.; Trubač, J.; Sracek, O.; Chrastný, V.; Mapani, B. S. Tracing the metal dynamics in semi-arid soils near mine tailings using stable Cu and Pb isotopes. *Chem. Geol.* **2019**, *515*, 61−76.
(48) Xia, Y.; Gao, T.; Liu, Y.; Wang, Z.; Liu, C.; Wu, Q.; Qi, M.; Lv, Y.; Li, F. Zinc isotope revealing zinc's sources and transport processes in karst region. *Sci. Total Environ.* **2020**, *724*, No. 138191.

(49) Liu, Y.; Gao, T.; Xia, Y.; Wang, Z.; Liu, C.; Li, S.; Wu, Q.; Qi, M.; Lv, Y. Using Zn isotopes to trace Zn sources and migration pathways in paddy soils around mining area. *Environ. Pollut.* **2020**, *267*, No. 115616.
(50) Liu, S.-A.; Wang, Z.; Li, S.; Huang, J.; Yang, W. Zinc isotope evidence for a large-scale carbonated mantle beneath eastern China. *Earth Planet. Sci. Lett.* **2016**, *444*, 169−178.
(51) Lv, Y.; Liu, S.; Zhu, J.; Li, S. Copper and zinc isotope fractionation during deposition and weathering of highly metalliferous black shales in central China. *Chem. Geol.* **2016**, *445*, 24−35.
(52) Liang, B.; Han, G.; Liu, M.; Li, X. Zn isotope fractionation during the development of low-humic gleysols from the Mun River Basin, northeast Thailand. *Catena* **2021**, *206*, No. 105565, DOI: 10.1016/j.catena.2021.105565.
(53) Moore, J. W.; Semmens, B. X. Incorporating uncertainty and prior information into stable isotope mixing models. *Ecol. Lett.* **2008**, *11* (5), 470−480.
(54) Lu, S.; Cai, W. Y.; Zhang, X. D.; Li, X. B.; Huang, H.; Zhang, F. F.; Zhang, J. Black coral as a new environmental recorder: The lead profiles in coral skeletons over the past century. *Mar. Pollut. Bull.* **2015**, *101* (1), 226−231.
(55) Wan, D.; Song, L.; Mao, X.; Yang, J.; Jin, Z.; Yang, H. One-century sediment records of heavy metal pollution on the southeast Mongolian Plateau: Implications for air pollution trend in China. *Chemosphere* **2019**, *220*, 539−545.
(56) Mohr, S.; Giurco, D.; Retamal, M.; Mason, L.; Mudd, G. Global Projection of Lead-Zinc Supply from Known Resources. *Resources* **2018**, *7* (1), 17.
(57) Lv, Y.; Liu, S.; Teng, F.; Wei, G.; Ma, J. Contrasting zinc isotopic fractionation in two mafic-rock weathering profiles induced by adsorption onto Fe (hydr)oxides. *Chem. Geol.* **2020**, *539*, No. 119504.
(58) Araújo, D. F.; Boaventura, G. R.; Machado, W.; Viers, J.; Weiss, D.; Patchineelam, S. R.; Ruiz, I.; Rodrigues, A. P. C.; Babinski, M.; Dantas, E. Tracing of anthropogenic zinc sources in coastal environments using stable isotope composition. *Chem. Geol.* **2017**, *449*, 226−235.
(59) Araújo, D. F.; Ponzevera, E.; Briant, N.; Knoery, J.; Sireau, T.; Mojtahid, M.; Metzger, E.; Brach-Papa, C. Assessment of the metal contamination evolution in the Loire estuary using Cu and Zn stable isotopes and geochemical data in sediments. *Mar. Pollut. Bull.* **2019**, *143*, 12−23.
(60) Araújo, D. F.; Machado, W.; Weiss, D.; Mulholland, D. S.; Garnier, J.; Souto-Oliveira, C. E.; Babinski, M. Zinc isotopes as tracers of anthropogenic sources and biogeochemical processes in contaminated mangroves. *Appl. Geochem.* **2018**, *95*, 25−32.
(61) Guinoiseau, D.; Bouchez, J.; Gelabert, A.; Louvat, P.; Moreira-Turcq, P.; Filizola, N.; Benedetti, M. F. Fate of particulate copper and zinc isotopes at the Solimoes-Negro river confluence, Amazon Basin, Brazil. *Chem. Geol.* **2018**, *489*, 1−15.
(62) Wensman, S. M.; Shiel, A. E.; McConnell, J. R. Lead isotopic fingerprinting of 250-years of industrial era pollution in Greenland ice. *Anthropocene* **2022**, *38*, No. 100340, DOI: 10.1016/j.ancene.2022.100340.
(63) Hosono, T.; Su, C. C.; Okamura, K.; Taniguchi, M. Historical record of heavy metal pollution deduced by lead isotope ratios in core sediments from the Osaka Bay, Japan. *J. Geochem. Explor.* **2010**, *107* (1), 1−8.
(64) Sakata, M.; Xu, H.; Mashio, A. S. Analysis of historical trend of pollution sources of lead in Tokyo Bay based on lead isotope ratios in sediment core. *J. Oceanogr.* **2018**, *74* (2), 187−196.
(65) Mukai, H.; Furuta, N.; Fujii, T.; Ambe, Y.; Sakamoto, K.; Hashimoto, Y. Characterization of Sources of Lead in the Urban Air of Asia Using Ratios of Stable Lead Isotopes. *Environ. Sci. Technol.* **1993**, *27* (7), 1347−1356.
(66) Bond, T. C.; Bhardwaj, E.; Dong, R.; Jogani, R.; Jung, S. K.; Roden, C.; Streets, D. G.; Trautmann, N. M. Historical emissions of black and organic carbon aerosol from energy-related combustion, 1850−2000. *Global Biogeochem. Cycles* **2007**, *21* (2), No. GB2018, DOI: 10.1029/2006GB002840.
(67) Mudd, G. M.; Jowitt, S. M.; Werner, T. T. The world's lead-zinc mineral resources: Scarcity, data, issues and opportunities. *Ore Geol. Rev.* **2017**, *80*, 1160−1190.
(68) Rauch, J. N.; Pacyna, J. M. Earth's global Ag, Al, Cr, Cu, Fe, Ni, Pb, and Zn cycles. *Global Biogeochem. Cycles* **2009**, *23* (2), No. GB2001, DOI: 10.1029/2008gb003376.
(69) Miller, H.; Croudace, I. W.; Bull, J. M.; Cotterill, C. J.; Dix, J. K.; Taylor, R. N. A 500 year sediment lake record of anthropogenic and natural inputs to Windermere (English Lake District) using double-spike lead isotopes, radiochronology, and sediment micro-analysis. *Environ. Sci. Technol.* **2014**, *48* (13), 7254−7263.
(70) Cheng, H.; Hu, Y. Planning for sustainability in China's urban development: status and challenges for Dongtan eco-city project. *J. Environ. Monit.* **2010**, *12* (1), 119−126.
(71) Calvo, G.; Valero, A.; Valero, A. Assessing maximum production peak and resource availability of non-fuel mineral resources: Analyzing the influence of extractable global resources. *Resour., Conserv. Recycl.* **2017**, *125*, 208−217.
(72) Morrison, W. M. *China's Economic Rise: History, Trends, Challenges, and Implications for the United States*; Congressional Research Service: Washington, DC, 2013.
(73) Mingram, J.; Allen, J. R. M.; Brüchmann, C.; Liu, J.; Luo, X.; Negendank, J. F. W.; Nowaczyk, N.; Schettler, G. Maar- and crater lakes of the Long Gang Volcanic Field (N.E. China)—overview, laminated sediments, and vegetation history of the last 900 years. *Quat. Int.* **2004**, *123*−*125*, 135−147.
(74) Li, H. B.; Yu, S.; Li, G. L.; Deng, H. Lead contamination and source in Shanghai in the past century using dated sediment cores from urban park lakes. *Chemosphere* **2012**, *88* (10), 1161−1169.
(75) Chen, J.; Tan, M.; Li, Y.; Zhang, Y.; Lu, W.; Tong, Y.; Zhang, G.; Li, Y. A lead isotope record of shanghai atmospheric lead emissions in total suspended particles during the period of phasing out of leaded gasoline. *Atmos. Environ.* **2005**, *39* (7), 1245−1253.
(76) Juillot, F.; Noël, V.; Gelabert, A.; Jouvin, D.; Göttlicher, P. J.; Belin, S.; Müller, B.; Morin, G.; Voegelin, A. Can Zn isotope in sediments record past eutrophication of freshwater lakes? A pilot study at Lake Baldegg (Switzerland). *Chem. Geol.* **2023**, *620*, No. 121321, DOI: 10.1016/j.chemgeo.2023.121321.
(77) Zhang, C.-X.; Sun, X.; Xie, S.; Xie, W.; Zhan, D. The phytoplankton of the Huguangyan Maar Lake (in Chinese). *Acta Hydrobiol. Sin.* **2009**, *32*, 620−630.
(78) Huang, Y. M.; Zhang, R. J.; Li, K. C.; Cheng, Z. N.; Zhong, G. C.; Zhang, G.; Li, J. Experimental Study on the Role of Sedimentation and Degradation Processes on Atmospheric Deposition of Persistent Organic Pollutants in a Subtropical Water Column. *Environ. Sci. Technol.* **2017**, *51* (8), 4424−4433.
(79) John, S. G.; Genevieve Park, J.; Zhang, Z.; Boyle, E. A. The isotopic composition of some common forms of anthropogenic zinc. *Chem. Geol.* **2007**, *245* (1−2), 61−69.
(80) Bigalke, M.; Weyer, S.; Kobza, J.; Wilcke, W. Stable Cu and Zn isotope ratios as tracers of sources and transport of Cu and Zn in contaminated soil. *Geochim. Cosmochim. Acta* **2010**, *74* (23), 6801−6813.
(81) Mattielli, N.; Petit, J. C. J.; Deboudt, K.; Flament, P.; Perdrix, E.; Taillez, A.; Rimetz-Planchon, J.; Weis, D. Zn isotope study of atmospheric emissions and dry depositions within a 5 km radius of a Pb−Zn refinery. *Atmos. Environ.* **2009**, *43* (6), 1265−1272.
(82) Dong, S.; Ochoa Gonzalez, R.; Harrison, R. M.; Green, D.; North, R.; Fowler, G.; Weiss, D. Isotopic signatures suggest important contributions from recycled gasoline, road dust and non-exhaust traffic sources for copper, zinc and lead in PM10 in London, United Kingdom. *Atmos. Environ.* **2017**, *165*, 88−98.
(83) Jeong, H.; Ryu, J. S.; Ra, K. Characteristics of potentially toxic elements and multi-isotope signatures (Cu, Zn, Pb) in non-exhaust traffic emission sources. *Environ. Pollut.* **2022**, *292* (Pt A), No. 118339.

(84) Wang, D.; Zheng, L.; Ren, M.; Li, C.; Dong, X.; Wei, X.; Zhou, W.; Cui, J. Zinc in soil reflecting the intensive coal mining activities: Evidence from stable zinc isotopes analysis. *Ecotoxicol. Environ. Saf.* **2022**, *239*, No. 113669.

https://doi.org/10.1021/acs.est.3c00511
Environ. Sci. Technol. 2023, 57, 15184−15192